Relationship of Membrane Curvature to the Formation of Pores by Magainin 2[†]

Katsumi Matsuzaki,*[,‡] Ken-ichi Sugishita,[‡] Noriko Ishibe,[‡] Mayu Ueha,[‡] Saori Nakata,[‡] Koichiro Miyajima,[‡] and Richard M. Epand[§]

Graduate School of Pharmaceutical Sciences, Kyoto University, Sakyo-ku, Kyoto 606-8501, Japan, and Department of Biochemistry, McMaster University, Hamilton, Ontario, L8N 3Z5, Canada

Received March 9, 1998; Revised Manuscript Received June 1, 1998

ABSTRACT: Magainin 2, an antimicrobial peptide from the *Xenopus* skin, kills bacteria by permeabilizing the cell membranes. We have proposed that the peptide preferentially interacts with acidic phospholipids to form a peptide−lipid supramolecular complex pore, which allows mutually coupled transbilayer traffic of ions, lipids, and peptides, thus simultaneously dissipating transmembrane potential and lipid asymmetry [Matsuzaki, K., Murase, O., Fujii, N., and Miyajima, K. (1996) *Biochemistry 35*, 11361−11368]. In this paper, we examined the effect of membrane curvature strain on pore formation. Magainin effectively forms the pore only in phosphatidylglycerol bilayers at low peptide-to-lipid ratios, well below 1/100. In contrast, the permeabilization of phosphatidylserine, phosphatidic acid, or cardiolipin bilayers occurred at much higher peptide-to-lipid ratios (1/50 to 1/10) with some morphological change of the vesicles. The latter three classes of phospholipids are known to form hexagonal II structures under conditions of reduced interlipid electrostatic repulsions. Incorporation of phosphatidylethanolamine also inhibited the magainin-induced pore formation in the inhibitory order of dioleoylphosphatidylethanolamine > dielaidoylphosphatidylethanolamine. Addition of a small amount of palmitoyllysophosphatidylcholine enhanced the peptide-induced permeabilization of phosphatidylglycerol bilayers. Magainin greatly raised the bilayer to hexagonal II phase transition temperature of dipalmitoleoylphosphatidylethanolamine. These results suggest that the peptide imposes positive curvature strain, facilitating the formation of a torus-type pore, and that the presence of negative curvature-inducing lipids inhibits pore formation.

Biological membranes usually contain more than 100 species of lipids with different polar groups and hydrophobic moieties, although reasons for the diversity are not well understood (*1*). The lipid composition regulates the local physicochemical properties of the membranes, such as surface charge, fluidity, and curvature strain, which in turn modulate the functions of membrane-associated peptides and proteins. For example, the presence of non-bilayer-forming lipids affects the activities of protein kinase C (*2*, *3*), rhodopsin (*4*), mycoplasma Mg^{2+}-ATPase, mitochondrial ubiquinol−cytochrome *c* reductase, and H^+-ATPase (*5*). Other examples include membranolytic peptides.

A number of membrane-acting peptides composed of 15−40 amino acid residues have been discovered in nature. They show cytotoxicity by permeabilizing the cell membranes of target cells, serving as offensive or defensive weapons (*6*−*10*). These peptides can apparently be classified into antimicrobial and hemolytic peptides. The former class of peptides selectively kills bacteria without exhibiting significant toxicity against host cells, thus being a promising candidate of novel antibiotics (*11*). There is accumulating evidence suggesting that the antimicrobial or self-defense peptides, which are usually highly basic, recognize acidic phospholipids exposed to the surface of bacterial membranes (*9*, *10*, *12*). On the other hand, their low hydrophobicity makes the affinity of these peptides for erythrocytes minimal, because the erythrocyte surface is exclusively composed of zwitterionic phospholipids, such as PC[1] and sphingomyelin (*13*).

Magainin 2 is a self-defense peptide isolated from the skin of the African frog, *Xenopus laevis* (*14*): GIGKFLHSAKKFGKAFVGEIMNS. We have proposed the mecha-

[†] Supported by the Naito Foundation, the Research Foundation for Pharmaceutical Sciences, and a Grant-in-Aid for Encouragement of Young Scientists (09771946) from the Ministry of Education, Science, and Culture of Japan as well as the Medical Research Council of Canada (MT-7654).

* To whom correspondence should be addressed. Telephone: 81-75-753-4574. Fax: 81-75-761-2698. E-mail: katsumim@pharm.kyoto-u.ac.jp.

[‡] Kyoto University.

[§] McMaster University.

[1] Abbreviations: 18L, GIKKFLGSIWKFIKAFVG; Ac-18A-NH_2, *N*-acetyl-DWLKAFYDKVAEKLKEAF-amide; BBPS, bovine brain L-α-phosphatidyl-L-serine; CD, circular dichroism; CL, cardiolipin; DEPE, dielaidoyl-L-α-phosphatidylethanolamine; DMPC, dimyristoyl-L-α-phosphatidylcholine; DMPG, dimyristoyl-L-α-phosphatidylglycerol; DOPE, dioleoyl-L-α-phosphatidylethanolamine; DPoPE, dipalmitoleoyl-L-α-phosphatidylethanolamine; DSC, differential scanning calorimetry; ECCL, *Escherichia coli* cardiolipin; EYPC, egg yolk L-α-phosphatidylcholine; EYPA, L-α-phosphatidic acid enzymatically converted from EYPC; EYPG, L-α-phosphatidyl-DL-glycerol enzymatically converted from EYPC; Fmoc, fluoren-9-ylmethoxycarbonyl; HPLC, high-performance liquid chromatography; LPC, palmitoyl-L-α-phosphatidylcholine; LUVs, large unilamellar vesicles; MLVs, multilamellar vesicles; L/P, lipid to peptide molar ratio; NBD-PE, *N*-[(7-nitrobenz-2-oxa-1,3-diazol-4-yl)]dipalmitoyl-L-α-phosphatidylethanolamine; PA, phosphatidic acid; PC, phosphatidylcholine; PE, phosphatidylethanolamine; PG, phosphatidylglycerol; POPG, palmitoyloleoyl-L-α-phosphatidyl-DL-glycerol; D-POPS, palmitoyloleoyl-L-α-phosphatidyl-D-serine; L-POPS, palmitoyloleoyl-L-α-phosphatidyl-L-serine; PS, phosphatidylserine; P/L, peptide to lipid molar ratio; Rho-PE, *N*-(lissamine Rhodamine B sulfonyl)dioleoyl-L-α-phosphatidylethanolamine; SUVs, small unilamellar vesicles; T_H, bilayer to hexagonal II phase transition temperature.

S0006-2960(98)00539-X CCC: $15.00
Published on Web 08/07/1998

nism of magainin-induced membrane permeabilization as follows [for review, see (*15*)]. The peptide preferentially binds to acidic phospholipids, forming an amphipathic helix (*16*). The helix essentially lies parallel to the membrane surface (*17, 18*). Five helices, on the average, together with several surrounding lipids form a membrane-spanning pore comprising a dynamic, peptide−lipid supramolecular complex, which allows not only ion transport but also rapid flip-flop of the membrane lipids (*19*). The pore-lining lipids make the otherwise insulated outer and inner leaflets a continuum (see also Figure 11A). The pore structure has been recently detected by in-plane neutron scattering (*20*). Upon the disintegration of the pore, a fraction of the peptide molecules stochastically translocates into the inner leaflet (*21, 22*). These processes can be controlled by modifying the peptide charge (*23*).

The lipid composition of the membrane is also an important modulating factor of magainin−lipid interactions. Aside from its preferential interaction with negatively charged lipids, magainin appears to discriminate among various acidic phospholipids. The peptide much more effectively permeabilizes EYPG bilayers than BBPS bilayers, although both lipids have net −1 charge and are in the fluid state at physiological temperatures. This observation suggests that the mechanism of membrane permeabilization can differ between these acidic phospholipid bilayers. However, little attention has been paid to this point. Investigators of antimicrobial peptide−lipid interactions have used PG (*21, 24, 25*), PS (*26*), and PA (*27*) as model acidic lipid, according to their preferences.

In this study, we compared the membrane-permeabilizing activity of F12W magainin 2, a fluorescent, equipotent analogue of magainin 2 (*18*), against four classes of acidic phospholipids. The effects of PE and LPC incorporation were also examined. We found that the membrane permeabilization mechanism strongly depends on the lipid composition. The results are discussed in terms of the curvature strain imposed by the peptide on the membrane and the pore structure.

MATERIALS AND METHODS

Materials. F12W magainin 2 was synthesized by a standard Fmoc-based solid phase method, as previously described (*18*). The purity of the synthesized peptide was determined by quantitative amino acid analysis, analytical HPLC, and ion spray mass spectroscopy. The peptide concentration was routinely determined on the basis of the tryptophan UV absorption (*28*). EYPG was a kind gift of Nippon Fine Chemical Co. (Takasago, Japan). POPG, L-POPS, D-POPS, DPoPE, and Rho-PE were purchased from Avanti Polar Lipids (Alabaster, AL). NBD-PE was a product of Molecular Probes (Eugene, OR). The other phospholipids were obtained from Sigma (St. Louis, MO). Calcein and spectrograde organic solvents were supplied by Dojindo (Kumamoto, Japan). All other chemicals from Wako (Tokyo, Japan) were of special grade. A Hepes−NaOH buffer (10 mM Hepes/150 mM NaCl/1 mM EDTA, pH 7.4) was prepared from water twice distilled in a glass still.

Vesicle Preparation. LUVs were prepared and characterized, as described elsewhere (*19*). Briefly, a lipid film, after being dried under vacuum overnight, was hydrated with a 70 mM calcein solution (pH was adjusted to 7.4 with NaOH) or the buffer and vortex-mixed to produce MLVs. The suspension was freeze−thawed for five cycles and then successively extruded through polycarbonate filters (a 0.6 μm pore size filter, 5 times, and then two stacked 0.1 μm pore size filters, 10 times). SUVs for CD measurements were produced by sonication of the freeze−thawed MLVs in ice/water under a nitrogen atmosphere (*16, 29*). A Tris-HCl buffer (10 mM Tris/150 mM NaCl/1 mM EDTA, pH 7.4) was used for the CD studies. The lipid concentration was determined in triplicate by phosphorus analysis (*30*).

Calcein Leakage. Calcein-entrapped vesicles were separated from free calcein on a Bio-gel A-1.5m column. In the case of PG membranes, calcein-free LUVs were mixed with the dye-loaded liposomes to adjust the lipid concentration to a desired value. The release of calcein from the LUVs was fluorometrically monitored on a Shimadzu RF-5000 spectrofluorometer at an excitation wavelength of 490 nm and an emission wavelength of 520 nm at 30 °C. The maximum fluorescence intensity corresponding to 100% leakage was determined by the addition of 10% w/v Triton X-100 (20 μL) to 2 mL of the sample. The apparent percent leakage value[2] was calculated according to $100 \times (F - F_0)/(F_t - F_0)$ (*31*). F and F_t denote the fluorescence intensity before and after the detergent addition, respectively. F_0 represents the fluorescence of the intact vesicle.

Lipid Mixing. 6.25 μM BBPS/EYPC/NBD-PE (2/1/0.015) LUVs were mixed with 6.25 μM BBPS/EYPC/Rho-PE (2/1/0.024) LUVs at 30 °C, and the fluorescence intensity of NBD-PE at 522 nm (excitation 450 nm) was monitored in the presence or absence of 1 μM F12W magainin 2 (*32*). To estimate artifacts due to direct peptide−probe interactions, we also carried out control experiments. The fluorescence intensity at 522 nm of 12.5 μM BBPS/EYPC/NBD-PE/Rho-PE (2/1/0.0075/0.012) LUVs was recorded in the presence or absence of 1 μM F12W magainin 2.

Peptide Binding. The binding affinity of the peptide for the membrane was determined on the basis of tryptophan fluorescence. Peptide solutions (3 μM) containing various amounts of LUVs were incubated at 30 °C overnight to reach a binding equilibrium. Fluorescence emission spectra, in the range of 300−400 nm, were measured on a Hitachi F-4500 spectrofluorometer using an excitation wavelength of 280 nm. The spectra were corrected for both wavelength-dependent effects (*33*) and intensity loss due to light scattering after subtraction of the corresponding blank spectra without the peptide. The latter correction was carried out by use of indoxyl sulfate (*18*).

CD Spectra. CD spectra were measured on a Jasco J-720 apparatus interfaced to an NEC PC-9801 microcomputer, using a 1 mm path-length quartz cell to minimize the absorbance due to buffer components. The instrumental outputs were calibrated with nonhygroscopic ammonium *d*-camphor-10-sulfonate (*34*). Eight scans were averaged for each sample. The averaged blank spectra (the vesicle suspension) were subtracted. The peptide and the lipid concentrations were 30 μM and 1−2 mM, respectively. The reported spectra were the average of 2−4 independent preparations and were those of the membrane-bound form

[2] To obtain the true percent leakage value, the lifetime of the pore formed in the bilayer should be determined (*31*).

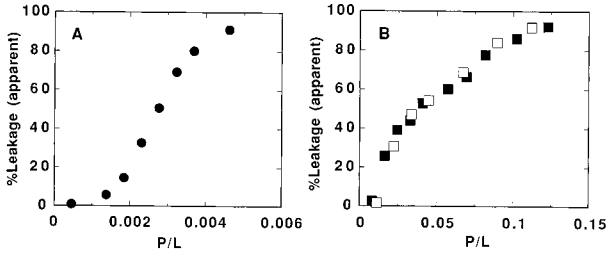

FIGURE 1: Magainin-induced permeabilization of PG and PS bilayers. F12W magainin 2 was added to calcein-entrapped LUVs. The dye release was fluorometrically detected at 30 °C. The apparent percent leakage values for 5 min are plotted as a function of P/L. (A) POPG; [lipid] = 100 μM. (B) (■) L-POPS; (□) D-POPS; [lipid] = 12.5 μM.

because further addition of vesicles caused no change in the spectra. The absence of any optical artifacts was confirmed elsewhere (*29*).

DSC. The peptide was dissolved in trifluoroethanol with a drop of water. Aliquots of this solution were added to a solution of DPoPE in chloroform/methanol (2/1, v/v). The solvent was evaporated under a stream of nitrogen to deposit the lipid as a film. Last traces of solvent were removed under vacuum for 2 h. The film was then hydrated with 20 mM PIPES/150 mM NaCl/1 mM EDTA/20 mg/L NaN_3. The vesicle suspension and the buffer (reference) were degassed under vacuum. The bilayer to hexagonal II phase transition temperature was measured on a MC-2 high-sensitivity differential scanning calorimeter (Microcal, Amherst, MA). The heating scan rate was 37 °C/h, and the lipid concentration was 10 mg/mL. Data were analyzed using the DA-2 software provided by the manufacturer by fitting the curves to the thermal transition of two independent components. The transition temperature, calorimetric enthalpy, and cooperativity of the theoretical curve were adjusted to give the best fit.

RESULTS

Comparison between POPG and POPS. To clarify the effect of the lipid headgroup on the magainin-induced membrane permeabilization, we used POPG and POPS having identical acyl chains. The permeabilization was estimated by use of the dye release assay. Figure 1 shows the percent leakage for a 5 min incubation as a function of P/L. In the case of POPG vesicles (Figure 1A), the addition of F12W magainin 2 caused dye efflux at lower P/L values, around 0.003. Furthermore, the dose−response curve was sigmoidal, suggesting the cooperative nature of pore formation. In contrast, L-POPS bilayers were much more resistant to the peptide-induced membrane permeabilization (Figure 1B, closed squares). Compared with POPG, about 10 times larger amounts of the peptide were required to induce a similar extent of dye release. Moreover, the cooperativity found in the POPG bilayers was lost. No discernible difference was observed between L-POPS and D-POPS (Figure 1B, closed vs open squares). Figure 2 exhibits the 90° light-scattering intensity of peptide-treated LUVs relative to that in the absence of the peptide (control). The addition of the peptide did not change the light-scattering intensity of POPG vesicles at P/L = 0.008, at a condition in which there is leakage (Figure 1A), indicating that neither micellization nor fusion of the liposomes occurs (upper trace). On the contrary, peptide treatment caused a rapid decrease and a subsequent gradual increase in the scattering intensity of L-POPS LUVs at a P/L value of 0.1 (lower trace), where a significant extent of dye release was observed (Figure 1B). Clearly, the magainin-induced permeabilization of the L-POPS bilayers accompanies some morphological change in the vesicles.

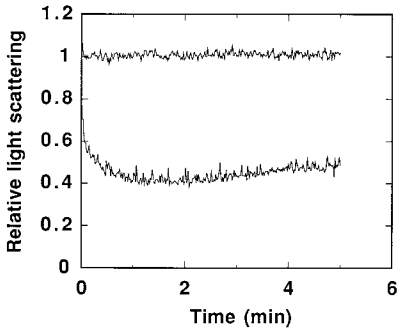

FIGURE 2: Magainin-induced morphological change in LUVs. The 90° light-scattering intensity of LUVs at 400 nm in the presence of F12W magainin 2 is represented as the value relative to the control value in the absence of the peptide. Upper trace: [POPG] = 100 μM, P/L = 0.008. Lower trace: [L-POPS] = 12.5 μM, P/L = 0.1.

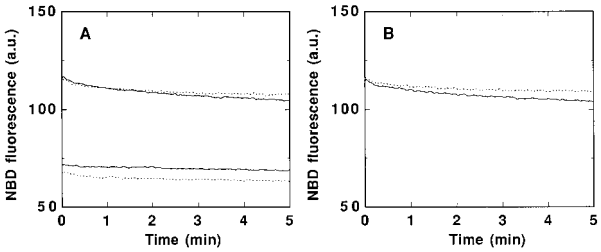

FIGURE 3: Lipid mixing assay. (A) Upper traces: 6.25 μM BBPS/EYPC/NBD-PE (2/1/0.015) LUVs were mixed with 6.25 μM BBPS/EYPC/Rho-PE (2/1/0.024) LUVs at 30 °C, and the fluorescence intensity of NBD-PE at 522 nm (excitation 450 nm) was monitored in the presence (solid trace) or absence (dotted trace) of 1 μM F12W magainin 2. Lower traces: The fluorescence intensity at 522 nm of 12.5 μM BBPS/EYPC/NBD-PE/Rho-PE (2/1/0.0075/0.012) LUVs was recorded in the presence (solid trace) or absence (dotted trace) of 1 μM F12W magainin 2. (B) The fluorescence intensity at 522 nm of 6.25 μM BBPS/EYPC/NBD-PE (2/1/0.015) LUVs was monitored in the presence (solid trace) or absence (dotted trace) of 0.5 μM F12W magainin 2.

Comparison between EYPG and BBPS or between EYPG/EYPC (2/1) and BBPS/EYPC (2/1) gave results similar to those presented in Figures 1 and 2. For example, the P/L values at which 50% dye leakage was observed were ca. 0.006 and 0.15 for the EYPG/EYPC and BBPS/EYPC systems, respectively (see also Figure 5).

Lipid Mixing. To elucidate the effect of magainin on the morphology of PS liposomes, we carried out the lipid mixing assay. F12W magainin 2 was added to an equimolar mixture of LUVs composed of BBPS and EYPC (2/1) containing either NBD-PE or Rho-PE at a P/L of 0.08. Only a slight decrease in NBD fluorescence was observed (upper traces, Figure 3A). If 100% lipid mixing had occurred, the fluorescence intensity would have been reduced to a much lower value indicated by the lower solid curve in Figure 3A where BBPS/EYPC LUVs colabeled with NBD-PE and Rho-PE were mixed with the peptide. The small fluorescence decrease is not due to a minor extent of peptide-induced lipid

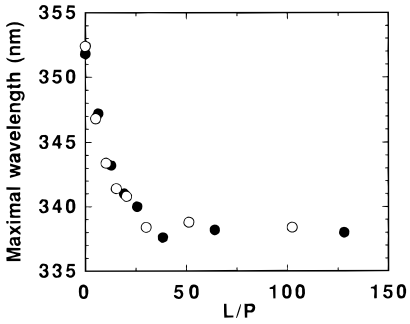

FIGURE 4: Binding affinity of F12W magainin 2 for negatively charged bilayers. A peptide solution (final concentration 3 μM) was incubated with various concentrations of EYPG/EYPC (2/1) LUVs (●) or BBPS/EYPC (2/1) LUVs (○) at 30 °C overnight. The maximal wavelength of Trp fluorescence is plotted as a function of L/P.

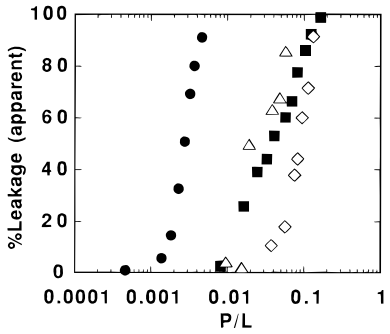

FIGURE 5: F12W magainin 2 induced release of calcein from various acidic phospholipid LUVs. The apparent percent calcein leakage values for 5 min are plotted as a function of P/L. (●) EYPG; (■) BBPS; (△) EYPA; (◇) ECCL.

mixing, but is attributable to an artifact arising from peptide−NBD interactions, because the addition of the peptide to the NBD-PE-labeled vesicles resulted in a similar extent of fluorescence reduction (Figure 3B).

Binding Affinity. The binding affinity of F12W magainin 2 for EYPG/EYPC (2/1) LUVs and BBPS/EYPC (2/1) LUVs was estimated on the basis of Trp fluorescence spectra. Figure 4 depicts the maximal fluorescence emission as a function of L/P while the peptide concentration was kept constant at 3 μM. Addition of the vesicles caused a blue shift, suggesting that the fluorophore is buried in a more hydrophobic environment of the bilayer. Irrespective of the lipid system, the shift reached a plateau value of 15 nm at L/P values above 25, where the peptide binding is complete. The change in wavelength with L/P, which is a measure of binding affinity, for the PG-based membranes was superimposable to that for the PS-based system. These results indicate that the affinity of the peptide for both bilayers is the same despite a large difference in susceptibility to the peptide-triggered membrane permeabilization.

Comparison among Various Acidic Phospholipids. Figure 5 compares the calcein release activity of F12W magainin 2 against various acidic phospholipid bilayers, including EYPG (closed circles), BBPS (closed squares), EYPA (open triangles), and ECCL (open diamonds). In the case of EYPG, dye release was observed at P/L values well below 0.01 (cf. Figure 1A). In contrast, much higher P/L values in the range of 0.1−0.01 were required to permeabilize the other bilayers.

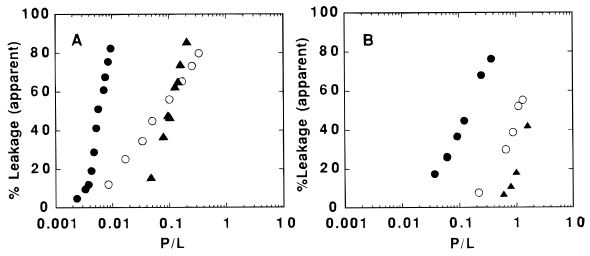

FIGURE 6: Effect of PE incorporation on magainin-induced membrane permeabilization. The apparent percent calcein leakage values at 5 min are plotted as a function of P/L. DEPE (○) or DOPE (▲) was substituted for EYPC in (A) EYPG/EYPC (2/1) LUVs (●) or (B) BBPS/EYPC (2/1) LUVs (●).

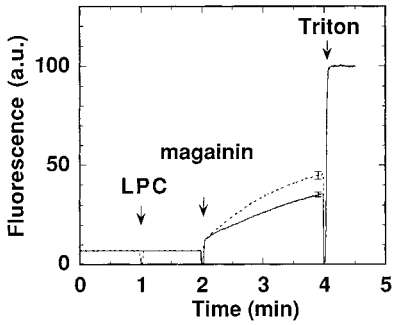

FIGURE 7: Effect of LPC on magainin-induced dye release. Calcein-loaded POPG LUVs were injected at time zero into the buffer preincubated at 30 °C. The final lipid concentration was 59 μM. Fluorescence intensity was continuously monitored at 520 nm (excitation at 490 nm). Addition of F12W magainin 2 at 2 min (P/L = 0.003) induced dye release, resulting in fluorescence increase (solid trace). In the case of the dashed trace, a sublytic concentration of LPC (0.98 μM) was pretreated at 1 min. The peptide-triggered calcein leakage was significantly sensitized.

Effect of PE Incorporation. Two kinds of PEs, DEPE and DOPE, were substituted for EYPC in EYPG/EYPC (2/1) LUVs or BBPS/EYPC (2/1) LUVs. Both PEs possess a double bond at position C9−C10, in each acyl chain, a trans one for DEPE and a cis one for DOPE. The cis double bond causes a much larger deviation of the acyl chain from the bilayer normal. The incorporation of the PEs inhibited the magainin-induced membrane permeabilization for both PG- and PS-based systems (Figure 6A and Figure 6B, respectively) in the inhibitory order of DOPE > DEPE.

Effect of LPC. Figure 7 shows the effects of LPC addition on the magainin-mediated dye release. POPG vesicles were injected at time zero into a buffer solution preincubated at 30 °C. Addition of F12W magainin 2 at 2 min enhanced the fluorescence intensity of calcein because of dye leakage (solid trace). The dashed trace indicates that pretreatment with a sublytic concentration of LPC at 1 min slightly but significantly sensitized magainin's effect. However, further addition of LPC inhibited the peptide-triggered membrane permeabilization (data not shown) probably because LPC expands the outer monolayer, inhibiting the binding of magainin, and/or because the peptide interacts with LPC free in solution. The latter was confirmed by the observation that LPC induced a blue shift of the Trp fluorescence of aqueous F12W magainin 2 (data not shown).

Figure 8 compares the lytic activity of LPC against POPG LUVs with that against POPS LUVs. The PS bilayers (dashed trace) were highly resistant to the detergent-mediated lysis. No leakage was observed at the highest LPC concen-

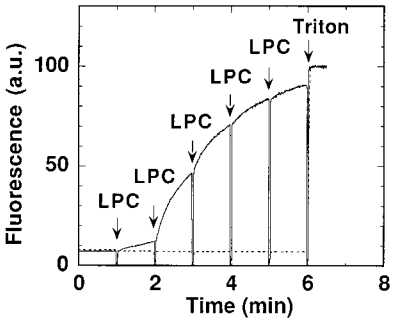

FIGURE 8: LPC-induced membrane permeabilization. Calcein-loaded POPG (solid trace) or POPS (dashed trace) LUVs were injected at time zero into the buffer preincubated at 30 °C. Fluorescence intensity was continuously monitored at 520 nm. Aliquots (10 μL) of 9.8 mM LPC solution were added to 2 mL of the sample every 1 min as indicated by the arrows. Triton X-100 was injected at 6 min to completely lyse the liposomes. The POPG and POPS concentrations were 3.4 and 4.5 μM, respectively.

Table 1: Molar Ellipticity of Membrane-Bound F12W Magainin 2 [a]

lipid	$[\theta]_{222}$ (deg·cm^2·dmol^{-1})	lipid	$[\theta]_{222}$ (deg·cm^2·dmol^{-1})
EYPG	$-23\,600 \pm 100$	ECCL	$-25\,300 \pm 400$
BBPS	$-24\,000 \pm 800$	EYPG/EYPC (2/1)	$-25\,200 \pm 800$
EYPA	$-23\,000 \pm 300$	BBPS/EYPC (2/1)	$-25\,500 \pm 300$

[a] The concentrations of the peptide and the lipid were 30 μM and 1−2 mM, respectively.

tration examined (24 μM). In contrast, the PG vesicles started to release the dye at the lowest LPC concentration (4.9 μM).

CD. The conformation of the peptide bound to membranes of various lipid compositions was estimated by use of CD. All the spectra exhibited double minima around 208 and 222 nm, characteristic of an α-helix, as reported previously (*23*). Table 1 summarizes the molar ellipticity values at 222 nm as a measure of the helicity. The values were in the narrow range of −23 000 to −25 500 deg cm^2 dmol^{-1}, corresponding to a helicity of 69−76%. No correlation was observed between the helicity and the dye-releasing activity (cf. Figure 5).

DSC. The effect of magainin 2 on membrane spontaneous curvature was evaluated on the basis of the effect of the peptide on the T_H of DPoPE (*25*). The pure lipid exhibited a T_H of 43 °C. The scans with added peptide showed a minor and a major peak (see Figure 9 for representative scans). This behavior is suggestive of separation of the membrane into domains rich in peptide (the major peak which is shifted to higher temperatures) and a peptide-depleted region. An analogous behavior has been observed with the related antimicrobial peptide, PGLa (*35*). The shift of the major peak was proportional to the amount of the peptide added up to about 0.2 mol % peptide. At higher peptide concentrations within the linear range, the minor peak was no longer discernible. The slope of the plot of T_H vs mole fraction of the added peptide was 1800 ± 300 (Figure 10).

DISCUSSION

Several mechanisms have been proposed for amphipathic peptide-induced membrane permeabilization, and considerable controversy still exists (*9*). Alamethicin forms the "barrel-stave channel", i.e., a bundle of membrane-spanning

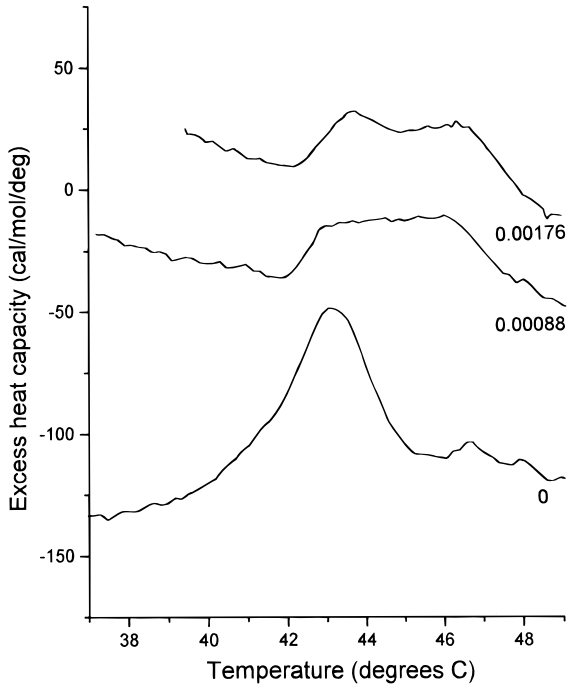

FIGURE 9: Representative DSC scans of DPoPE: The heating scan rate was 37 °C/h. The numbers on the ordinate are shown for scaling purposes. The positions of the various scans along this axis are arbitrary. Each scan is labeled with the mole fraction of magainin 2 which is mixed with the lipid. The scan marked 0 represents pure lipid.

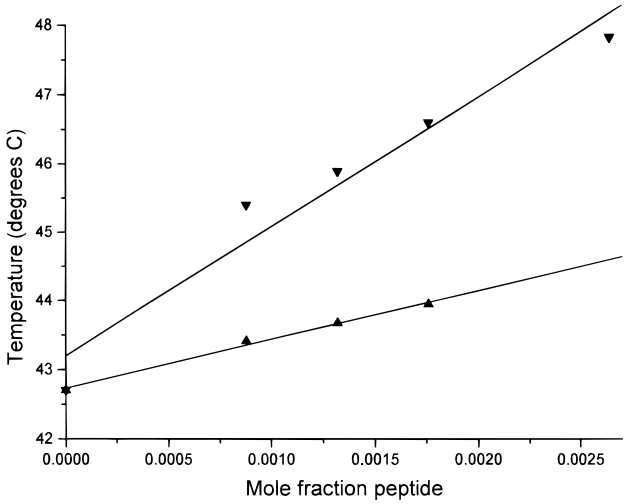

FIGURE 10: Dependence of T_H on the mole fraction of magainin 2. The upper curve (▼) corresponds to the transition temperature of the fitted peaks for the higher melting major component, while the lower curve (▲) gives the transition temperature of the fitted peak for the lower melting component which is suggested to be a peptide-depleted domain.

helices aligned with the polar side chains oriented toward the center (*36*). Cecropin and dermaseptin are suggested to disrupt bilayer organization by the "carpet-like mechanism", where a monolayer of surface-lying peptides covers the membrane surface (*37*). Ac-18A-NH_2 and 18L model peptides deteriorate bilayer barrier property by imposing positive and negative curvature strain on the membrane, respectively (*8, 38, 39*). These peptides are model amphiphathic helices of the plasma apolipoprotein A-I and of cytolytic peptides, respectively. We have proposed that magainin permeabilizes PG-based bilayers by forming a

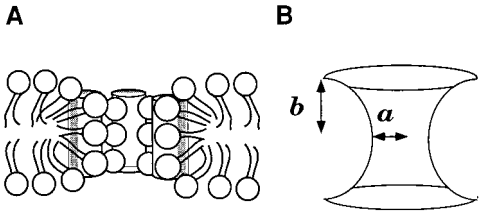

FIGURE 11: Model for magainin−lipid supramolecular complex pore. (A) The helical peptide molecules are illustrated as smaller cylinders. Spheres aligned between the helices represent the lipid headgroups. Shaded and open zones correspond to hydrophobic and hydrophilic regions, respectively. (B) The torus-type pore is characterized by two curvatures, which can be described by the radius of the narrowest part of the pore, *a*, and the lipid monolayer thickness, *b*.

peptide−lipid supramolecular pore as shown in Figure 11A (*19*, *21*). It is highly probable that the permeabilization mechanism of these peptides depends not only on the peptide structure but also on the lipid composition and therefore the physicochemical properties of the membrane. However, there have been relatively few systematic studies on this subject.

The mechanism of dye release for PS vesicles is different from that for PG vesicles, the latter being the cooperative supramolecular pore formation (*19*). The permeabilization of PS bilayers occurs at much higher P/L values without cooperativity (Figures 1 and 5) accompanying some morphological change of the vesicles (Figure 2). The small cooperativity (Hill coefficient, 1.7) of the ion channel formation of magainin 2 was also observed in PS/PE planar bilayers (*40*). The nature of the morphological change is presently unclear, but it does not involve vesicular fusion because no lipid mixing was detected (Figure 3). Our preliminary experiments using dark-field microscopy show that magainin induces a very complicated reorganization of PS giant oligolamellar vesicles which does not include any intervesicular interaction. It should be noted that the morphology of PG-based vesicles is also no longer intact at higher P/L values around 0.1 (data not shown).

We found no difference in the binding affinity of F12W magainin 2 between PG and PS (Figure 4), corroborating the idea that electrostatic interactions play a dominant role in the binding process (*16*, *41*). The penetration depth of the Trp residue does not significantly depend on the lipid headgroup because the blue shift of the fluorescence emission was the same in both the PG- and PS-based bilayers (Figure 4). The peptide conformation was also independent of the lipid species (Table 1). Therefore, the difference in the susceptibility of the membrane to magainin-induced permeabilization is a consequence of some difference in the pore-forming process. PS bilayers can resist pore formation and accumulate a large number of peptides on the surface, resulting in a reorganization of the bilayer. We observed similar phenomena in the case of tachyplesin I (*42*) and PGLa (unpublished work). In this regard, the carpet-like mechanism proposed by the group of Shai may correspond to the mechanism when PS is used as the acidic phospholipid (*26*).

Comparison among the four acidic phospholipids indicates that PG is the only lipid which is highly susceptible to magainin-induced pore formation (Figure 5). A unique character of PG compared with other acidic phospholipids has been also reported for gramicidin S−lipid interactions (*43*). The facts that PG and CL having the same headgroup behave differently and that there is no difference in the peptide-induced dye leakage between L-POPS and D-POPS (Figure 1B) suggest that some physicochemical properties of the bilayers, rather than specific molecular recognition of the headgroup structure by the peptide, regulate pore formation. PS, PA, and CL, but not PG, are known to form the hexagonal II phase under conditions of reduced interlipid electrostatic repulsions (*44*−*46*). The binding of polycationic magainin would locally reduce electrostatic repulsions between surrounding PS, PA, or CL molecules, thus imposing negative curvature strain on the membrane.

On the other hand, magainin 2 (Figures 9 and 10) as well as magainin analogues (*25*) significantly raise the T_H value of DPoPE, suggesting that in the absence of electrostatic effects the peptides impose positive curvature strain on the membrane. Ludtke et al. found that the magainin helix lies in the headgroup region of the bilayer, inducing membrane-thinning (*47*). This can be also interpreted as increasing positive curvature. These observations argue for our pore model (Figure 11A): A high positive curvature in a dimension perpendicular to the bilayer plane is required to stabilize the pore structure. Therefore, magainin cannot form the supramolecular complex in bilayers with higher negative curvature strain. Indeed, the incorporation of PEs inhibited pore formation. The inhibition by DOPE (T_H = 10 °C) is greater than that by DEPE (T_H = 65 °C). Both of these observations are consistent with these lipids inhibiting the formation of a pore with positive curvature (Figure 6). The smaller slope of the dose−response curve for the DEPE-containing membranes may be ascribed to the membrane-solidifying effect of this lipid which has a gel to liquid-crystalline phase transition at 37 °C as a pure lipid. The slope of these plots is related to the stability of the pore, suggesting that the pore with DEPE is relatively more stable (*22*).

The results of the LPC experiments further corroborate our hypothesis. Addition of a sublytic concentration of cone-shaped LPC, which imposes a positive curvature strain, facilitates magainin's leakage activity (Figure 7). Interestingly, PS bilayers are also much more resistant to LPC-induced lysis than PG bilayers, suggesting a similarity of the effects of magainin and of LPC (Figure 8).

A closer inspection of the pore structure (Figure 11) reveals that the pore-lining lipids would exhibit a negative curvature in a dimension parallel to the membrane plane. The balance between positive and negative curvature would depend on the pore size (*a* in Figure 11B), larger pores having predominantly positive curvature (*48*). Quantitatively, the membrane-bending energy, *W*, required for the formation of the torus pore depends on the spontaneous curvature, H_0, according to the following equation (*49*):

$$\frac{\partial W}{\partial H_0} \propto -2\pi a - 2(\pi - 4)b$$

If b = 2 nm, the right-hand side of the above equation becomes negative at values of a above 0.55 nm. The magainin pore allows the passage of calcein but not trypsin (*21*). The shape of the dye can be approximated by a 2 nm × 1 nm oblate ellipsoid, whereas the dimension of the enzyme is 5 nm × 4 nm × 4 nm (*50*). The neutron-

scattering experiment estimated that the size of the magainin pore formed in DMPG/DMPC (1/3) bilayers is 3 nm at a P/L value of 1/20 (*20*), although it may depend on P/L (*51*). Taken together, the diameter of the magainin pore is estimated to be 2−3 nm. Therefore, positive curvature facilitates the pore formation.

Membrane lytic peptides can be classified into two groups in terms of their effects on membrane curvature. One induces a negative curvature strain, decreasing the T_H value of DPoPE. A representative example, 18L, causes fusion of PC vesicles, and the addition of PE accelerates this process (*39*). A linear analogue of cyclic tachyplesin I also changes vesicle morphology, which is facilitated by PE incorporation (*24*). The other group, including magainin, imposes a positive curvature strain, increasing the T_H value. The pore formation by alamethicin, which induces membrane-thinning, is inhibited by the incorporation of PE (*52*). The membrane permeabilization triggered by Ac-18A-NH_2, a class A peptide, is again protected by the presence of PE (*39*). Class A peptides micellize PC bilayers at higher P/L values (*53*). Cyclic tachyplesin I having a micellization activity (*54*) is similarly counteracted by PE (*24*).

In this regard, melittin, a bee venom peptide, exhibits a unique character. The peptide appears to impose positive curvature strain on zwitterionic phospholipids. It micellizes PC vesicles (*55*) and converts the hexagonal II structure of PE to a bilayer (*56*). In contrast, the peptide penetrates more deeper into acidic phospholipids (*57*), inducing the hexagonal II phase with PA and CL bilayers, but not against PG vesicles (*58, 59*). We suggest that there are two opposing curvature effects of melittin on anionic lipids. One is the formation of pores with positive curvature as observed with zwitterionic membranes. However, with anionic lipids, charge neutralization by cationic melittin can promote negative curvature. With anionic lipids such as PA and CL, that readily form inverted phases under conditions of headgroup charge neutralization, the latter effect predominates. The fact that the melittin helix is more perpendicularly inserted in PS bilayers than PC or PG bilayers (*60*) further suggests that PG behaves differently from PS.

We reported that melittin translocates across PC-rich bilayers by transiently forming a pore, like magainin (*51*). The presence of anionic phospholipids inhibits pore formation, but the inhibitory effect of PG is weaker than that of PA (*61*). These observations can be explaind by the positive curvature associated with the pore formation in PC by melittin being inhibited by lipids, such as PA, which have negative curvature tendencies in the presence of melittin.

In the above discussion, we have explained pore formation by several peptides in various lipid bilayers from a point of view of the effect of the peptide on the spontaneous curvature of the membrane. That is, we considered the term of elastic bending energy containing the bending rigidity (*49*). However, the energy also includes a contribution from the modulus of Gaussian curvature, whose sign and magnitude are unknown. Furthermore, peptide-induced lowering of the rupture tension of the membrane has also been reported (*62*). Some of these other factors are likely to contribute to the observed differences in the behavior of different lytic peptides. However, for a particular peptide, its effect on the spontaneous curvature of a bilayer accurately predicts how differences in the spontaneous curvature of lipids will modulate the probability of pore formation.

In conclusion, the action of magainin is found to be quite sensitive to the lipid composition of the bilayers. Pore formation effectively occurs only in PG bilayers, which do not strongly counteract the peptide-induced positive curvature strain. In membranes with higher negative curvature strain, the bilayers can accumulate a large number of peptides on the outer leaflets without forming the pore, resulting in the bilayer reorganization. Thus, our study shows that the physicochemical properties of the membrane are also an important modulator of peptide−lipid interactions.

REFERENCES

1. Gennis, R. B. (1989) *Biomembranes; Molecular Structure and Function*, Springer-Verlag, New York.
2. Epand, R. M. (1992) in *Protein Kinase C. Current Concepts and Future Perspectives* (Lester, D. S., and Epand, R. M., Eds.) pp 135−156, Ellis Horwood, Chichester.
3. Zidovetzki, R. (1997) in *Lipid Polymorphism and Membrane Properties* (Epand, R. M., Ed.) pp 255−283, Academic Press, San Diego.
4. Brown, M. F. (1997) in *Lipid Polymorphism and Membrane Properties* (Epand, R. M., Ed.) pp 285−356, Academic Press, San Diego.
5. Yang, F. Y., and Hwang, F. (1996) *Chem. Phys. Lipids 81*, 197−202.
6. Cornut, I., Thiaudiére, E., and Dufourcq, J. (1993) in *The Amphipathic Helix* (Epand, R. M., Ed.) pp 173−220, CRC Press, Boca Raton.
7. Saberwal, G., and Nagaraj, R. (1994) *Biochim. Biophys. Acta 1197*, 109−131.
8. Epand, R. M., Shai, Y., Segrest, J. P., and Anantharamaiah, G. M. (1995) *Biopolymers 37*, 319−338.
9. Lohner, K., and Epand, R. M. (1997) *Adv. Biophys. Chem. 6*, 53−66.
10. Matsuzaki, K. (1998) in *Biomembrane Structures* (Chapman, D., and Haris, P., Eds.) pp 205−227, IOS Press, Amsterdam.
11. Boman, H. G., Marsh, J., and Goode, J. A. (1994) *Antimicrobial Peptides*, John Wiley and Sons, Chichester.
12. Matsuzaki, K., Sugishita, K., Fujii, N., and Miyajima, K. (1995) *Biochemistry 34*, 3423−3429.
13. Verkleij, A. J., Zwaal, R. F. A., Roelofsen, B., Comfurius, P., Kastelijn, D., and Deenen, L. L. M. V. (1973) *Biochim. Biophys. Acta 323*, 178−193.
14. Zasloff, M. (1987) *Proc. Natl. Acad. Sci. U.S.A. 84*, 5449−5453.
15. Matsuzaki, K. (1998) *Biochim. Biophys. Acta* (in press).
16. Matsuzaki, K., Harada, M., Funakoshi, S., Fujii, N., and Miyajima, K. (1991) *Biochim. Biophys. Acta 1063*, 162−170.
17. Bechinger, B., Zasloff, M., and Opella, S. J. (1993) *Protein Sci. 2*, 2077−2084.
18. Matsuzaki, K., Murase, O., Tokuda, H., Funakoshi, S., Fujii, N., and Miyajima, K. (1994) *Biochemistry 33*, 3342−3349.
19. Matsuzaki, K., Murase, O., Fujii, N., and Miyajima, K. (1996) *Biochemistry 35*, 11361−11368.
20. Ludtke, S. J., He, K., Heller, W. T., Harroun, T. A., Yang, L., and Huang, H. W. (1996) *Biochemistry 35*, 13723−13728.
21. Matsuzaki, K., Murase, O., Fujii, N., and Miyajima, K. (1995) *Biochemistry 34*, 6521−6526.
22. Matsuzaki, K., Murase, O., and Miyajima, K. (1995) *Biochemistry 34*, 12553−12559.
23. Matsuzaki, K., Nakamura, A., Murase, O., Sugishita, K., Fujii, N., and Miyajima, K. (1997) *Biochemistry 36*, 2104−2111.
24. Matsuzaki, K., Yoneyama, S., Fujii, N., Miyajima, K., Yamada, K., Kirino, Y., and Anzai, K. (1997) *Biochemistry 36*, 9799−9806.
25. Wieprecht, T., Dathe, M., Epand, R. M., Beyermann, M., Krause, E., Maloy, W. L., MacDonald, D. L., and Bienert, M. (1997) *Biochemistry 36*, 12869−12880.
26. Gazit, E., Boman, A., Boman, H. G., and Shai, Y. (1995) *Biochemistry 34*, 11479−11488.

27. Silvestro, L., Gupta, K., Weiser, J. N., and Axelsen, P. H. (1997) *Biochemistry 36*, 11452−11460.
28. Gill, S. C., and von Hippel, P. H. (1989) *Anal. Biochem. 182*, 319−326.
29. Matsuzaki, K., Nakai, S., Handa, T., Takaishi, Y., Fujita, T., and Miyajima, K. (1989) *Biochemistry 28*, 9392−9398.
30. Bartlett, G. R. (1959) *J. Biol. Chem. 234*, 466−468.
31. Schwarz, G., and Arbuzova, A. (1995) *Biochim. Biophys. Acta 1239*, 51−57.
32. Düzgüneş, N., Allen, T. M., Fedor, J., and Papahadjopoulos, D. (1987) *Biochemistry 26*, 8435−8442.
33. Melhuish, W. H. (1962) *J. Opt. Soc. Am. 52*, 1256−1258.
34. Takakuwa, T., Konno, T., and Meguro, H. (1985) *Anal. Sci. 1*, 215−218.
35. Latal, A., Degovics, G., Epand, R. F., Epand, R. M., and Lohner, K. (1997) *Eur. J. Biochem. 248*, 938−946.
36. Sansom, M. S. P. (1991) *Prog. Biophys. Mol. Biol. 55*, 139−235.
37. Shai, Y. (1995) *Trends Biol. Sci. 20*, 460−465.
38. Tytler, E. M., Segrest, J. P., Epand, R. M., Nie, S.-Q., Epand, R. F., Mishra, V. K., Venkatachalapathi, Y. V., and Anantharamaiah, G. M. (1993) *J. Biol. Chem. 29*, 22112−22118.
39. Polozov, I. V., Polozova, A. I., Tytler, E. M., Anantharamaiah, G. M., Segrest, J. P., Wooley, G. A., and Epand, R. M. (1997) *Biochemistry 36*, 9237−9245.
40. Cruciani, R. C., Barker, J. L., Durell, S. R., Raghunathan, G., Guy, H. R., Zasloff, M., and Stanley, E. F. (1992) *Eur. J. Pharmacol., Mol. Pharmacol. Sect. 226*, 287−296.
41. Vaz Gomes, A., de Waal, A., Berden, J. A., and Westerhoff, H. V. (1993) *Biochemistry 32*, 5365−5372.
42. Matsuzaki, K., Fukui, M., Fujii, N., and Miyajima, K. (1991) *Biochim. Biophys. Acta 1070*, 259−264.
43. Prenner, E. J., Lewis, R. N. A. H., Neuman, K. C., Gruner, S. M., Kondejewski, L. H., Hodges, R. S., and McElhaney, R. N. (1997) *Biochemistry 36*, 7906−7916.
44. Hope, M. J., and Cullis, P. R. (1980) *Biochem. Biophys. Res. Commun. 92*, 846−852.
45. Farren, S. B., Hope, M. J., and Cullis, P. R. (1983) *Biochem. Biophys. Res. Commun. 111*, 675−682.
46. Seddon, J. M., Kaye, R. D., and Marsh, D. (1983) *Biochim. Biophys. Acta 734*, 347−352.
47. Ludtke, S., He, K., and Huang, H. (1995) *Biochemistry 34*, 16764−16769.
48. Epand, R. M. (1998) *Biochim. Biophys. Acta* (in press).
49. Kabalnov, A., and Wennerström, H. (1996) *Langmuir 12*, 276−292.
50. Squire, P. G., and Himmel, M. E. (1979) *Arch. Biochem. Biophys. 196*, 165−177.
51. Matsuzaki, K., Yoneyama, S., and Miyajima, K. (1997) *Biophys. J. 73*, 831−838.
52. Heller, W. T., He, K., Ludtke, S. J., Harroun, T. A., and Huang, H. W. (1997) *Biophys. J. 73*, 239−244.
53. Epand, R. M., Gawish, A., Iqbal, M., Gupta, K. B., Chen, C. H., Segrest, J. P., and Anantharamaiah, G. M. (1987) *J. Biol. Chem. 262*, 9389−9396.
54. Matsuzaki, K., Nakayama, M., Fukui, M., Otaka, A., Funakoshi, S., Fujii, N., Bessho, K., and Miyajima, K. (1993) *Biochemistry 32*, 11704−11710.
55. Dufourcq, J., Faucon, J.-F., Fourche, G., Dasseux, J.-L., Le Maire, M., and Gulik-Krzywicki, T. (1986) *Biochim. Biophys. Acta 859*, 33−48.
56. Batenburg, A. M., van Esch, J. H., and de Kruijff, B. (1988) *Biochemistry 27*, 2324−2331.
57. Batenburg, A. M., Hibbeln, J. C. L., and de Kruijff, B. (1987) *Biochim. Biophys. Acta 903*, 155−165.
58. Batenburg, A. M., Hibbeln, J. C. L., Verkleij, A. J., and de Kruijff, B. (1987) *Biochim. Biophys. Acta 903*, 142−154.
59. Batenburg, A. M., van Esch, J. H., Leunissen-Bijvelt, J., Verkleij, A. J., and deKruijff, B. (1987) *FEBS Lett. 223*, 148−154.
60. De Jongh, H. H. J., Goormaghtigh, E., and Killian, J. A. (1994) *Biochemistry 33*, 14521−14528.
61. Benachir, T., and Lafleur, M. (1995) *Biochim. Biophys. Acta 1235*, 452−460.
62. Evans, E., and Needham, D. (1987) *J. Phys. Chem. 91*, 4219−4228.

BI980539Y